A Flexible Iterative Method for 3D Reconstruction from X-ray Projections

Laurent Launay*† Pierre Bouchet* Eric Maurincomme† Marie-Odile Berger* Jean-Laurent Mallet*

*CRIN – CNRS
Campus scientifique, B.P. 239
54506 Vandœuvre-lès-Nancy CEDEX, France

†General Electric Medical Systems
283 rue de la Minière, B.P. 34
78533 Buc CEDEX, France

E-mail: [launay,bouchet,berger,mallet]@loria.fr ericm@gemse.fr

Abstract

The problem of reconstructing a three-dimensional image of an object from a few number of X-ray projections is highly underdetermined. We propose a flexible method based on the regularization of the inverse linear problem with a general quadratic criterion. The minimization is performed by an iterative algorithm with a Gauss-Seidel behaviour. Thanks to the Discrete Smooth Interpolation (DSI) formulation, additional linear constraints are inserted, and the method is ensured to converge to the unique minimum. The application of this method is shown for 3D reconstruction of cerebral blood vessels from six projections, and the effect of various criteria is compared to the result of other algebraic methods.

1. Introduction

Recovering a three-dimensional image of an object from a number of X-ray projections is of major interest in many fields, and especially in medicine. In Digital Subtraction Angiography (DSA) the superimposition of blood vessels branches on projected images makes their relative position in space difficult to understand. Thus, for complex vessel networks such as the ones present in the brain, a three-dimensional image can be very useful to the diagnosis.

In X-ray projection images, a pixel represents the sum of a density function (the absorption coefficient of the object) over the line going from the X-ray source to this pixel. Different methods have been developed to reconstruct a 3D image of a vascular network from DSA images, depending on the number and the nature of the available projections. When dealing with only two orthogonal projections, one must use additional information or a strong a priori model. For coronary arteries, missing information can be retrieved thanks to cardiac movement [1]. In some cases, a geometric model based on the characteristics of the vessels [2] can be used. The flow information of the contrast agent propagation in the vessels can also help the reconstruction [5]. Binarity hypotheses have also been used [12] to reconstruct vessels from two or three projections, sometimes associated with simulated annealing [11]. Nevertheless, when a pathology such as an aneurysm or an Arteriovenous Malformation (AVM) is present in the images, such models cannot be used and a fully tomographic reconstruction is usually necessary.

The algebraic formulation has been widely used for solving 3D tomography problems [3]. The object space is discretized in cubic voxels, and the problem is transformed into the resolution of a huge linear system:

$$\mathbf{Y} = \mathbf{H}\mathbf{f} \tag{1}$$

The unknown N-dimensional vector $\mathbf{f}$ represents the density for all voxels, and the M-dimensional data vector $\mathbf{Y}$ contains all the pixels of the P projection images. The cone-beam projection process can be seen as a sparse $(M \times N)$ matrix $\mathbf{H}$ where each row $\mathbf{h}_j$ corresponds to the equation of one ray. The size of this system makes standard inversion techniques intractable; it can be solved by use of relaxation iterative methods that only require storage of vector $\mathbf{Y}$ and vector $\mathbf{f}$. The basics and the properties of such iterative algorithms are reviewed in section 2. Those algebraic methods are preferred when a large number of projections is available. A multiscale reconstruction scheme has also been devised to give efficient high-resolution 3D images [14].

Those methods sometimes suffer from a lack of flexibility when the number of projections is low (from 4 to 6). In section 3, we present another iterative method inspired from discrete constrained interpolation. This method allows to minimize with a Gauss-Seidel approach a general criterion composed of quadratic terms. Various forms of the criterion are proposed which correspond to different kinds of regularization of the ill-posed inverse problem. In section 4, the algorithm is applied to cerebral vascular reconstruction from six projections, and the effect of different criteria is compared to the solution given by classic algebraic methods.

2. Classic iterative methods

The ART (Algebraic Reconstruction Technique) algorithm for reconstruction from projections is based on the iterative formula for a given ray j:

$$f_i^{(n+1)} = f_i^{(n)} + \lambda^{(n)} \frac{y_j - \mathbf{h}_j \cdot \mathbf{f}^{(n)}}{\|\mathbf{h}_j\|^2} h_{ji} \qquad (2)$$

ART is a row-action technique since for each iteration, the volume is updated according to a different row of matrix $\mathbf{H}$. One cycle is completed when the M rays have been processed. If the linear system is consistent and if the relaxation coefficient is always comprised between 0 and 2, ART is known to converge to the minimum variance solution of (1), which is also the minimum norm solution [4]. If the system is inconsistent, the algorithm can be stopped after a few iterations, in order to give a suitable reconstruction.

MART (Multiplicative ART) is identical to ART except that the volume is updated multiplicatively instead of additively:

$$f_i^{(n+1)} = f_i^{(n)} \cdot \left(\frac{y_j}{\mathbf{h}_j \cdot \mathbf{f}^{(n)}} \right)^{\lambda^{(n)} h_{ji}} \qquad (3)$$

It has been proven [7] that if the system is consistent and if the volume is properly initialized, MART converges to the maximum entropy solution of (1).

3. Proposed algorithm

In most of the algebraic methods, a particular minimum of $\|\mathbf{Y} - \mathbf{Hf}\|$ is selected. Moreover, when data are noisy, the convergence of ART and MART is not insured. Appropriate relaxation coefficients and number of iterations must then be selected in order to avoid oscillatory effects.

Regularization methods have been used to solve complex 3D recovery problems [13]. In our case, quadratic terms are preferred to keep the convergence and the efficiency of the method. The approach we propose is based on a regularization of the inverse problem by a smoothness function and more generally by extending the criterion with any linear term. Our method uses the Discrete Smooth Interpolation (DSI) formulation, which furnishes a general tool for solving a large system of equations. The resolution is done by a Gauss-Seidel iterative approach where here again, only the volume and the projections need to be stored in computer memory.

In this section, we first review the basics of DSI algorithm and its convergence properties. Secondly, we show that it can be applied to the reconstruction problem. Finally, we enumerate some additional constraints that can be used to make the algorithm converge to a wide variety of solutions.

3.1. Discrete Smooth Interpolation

DSI was introduced by Mallet [8] as a generic algorithm to smoothly interpolate data from various origins. We consider a function φ defined on the set $\Omega = \{1, 2, \ldots, N\}$ indexing the nodes of a given graph G. Typically, G can model a surface composed of polygonal facets and φ represents the position of each vertex. In image processing, G can represent a regular discretization of a volume in cubic voxels, and φ the grey level. We consider here the case where φ has to be evaluated over the whole set Ω. We denote $N(\alpha)$ a neighbourhood of node α defined as the set of nodes that can be reached from α in less than a given number s of steps in graph G. $\Lambda(\alpha)$ is the orbit of α, defined as $N(\alpha) - \{\alpha\}$.

The DSI problem is to find φ which minimizes $R^*(\varphi) = R(\varphi) + \rho(\varphi)$, where R quantifies the roughness and ρ the violation of a set C of weighted linear constraints. These two terms are defined as:

$$\begin{aligned} R(\varphi) &= \sum_k \left| \sum_{\alpha \in N(k)} v^\alpha(k) \varphi(k) \right|^2 \\ \rho(\varphi) &= \sum_{c \in C} \varpi_c^2 \left| \mathbf{A}_c \varphi - b_c \right|^2 \end{aligned} \qquad (4)$$

$\{v^\alpha(k)\}$ are given weighting coefficients which correspond to a planarity constraint. They are supposed to verify $v^\alpha(k) > 0$ if $\alpha \in \Lambda(k)$, and $v^k(k) = -\sum_{\alpha \in \Lambda(k)} v^\alpha(k)$ otherwise.

The linear constraints c are $\sum_k \mathbf{A}_c(k)\varphi(k) = b_c$, and ϖ_c is their associated "certainty factor".

When considering a single node α, the resolution of $\frac{\partial R^*(\varphi)}{\partial \varphi(\alpha)} = 0$ leads to the following formula (called the local form of the DSI equation):

$$\varphi(\alpha) = -\frac{\Gamma^*(\alpha) + \sum_c \Gamma_c(\alpha)}{M^*(\alpha) + \sum_c \gamma_c(\alpha)} \qquad (5)$$

$$\begin{aligned} \Gamma^*(\alpha) &= \sum_{k \in N(\alpha)} v^\alpha(k) \sum_{\beta \in \Lambda(k)} v^\beta(k) \varphi(\beta) \\ M^*(\alpha) &= \sum_{k \in N(\alpha)} v^\alpha(k)^2 \\ \gamma_c(\alpha) &= \varpi_c^2 A_c(\alpha)^2 \\ \Gamma_c(\alpha) &= \varpi_c^2 A_c(\alpha) \left(\sum_{\beta \neq \alpha} A_c(\beta) \varphi(\beta) - b_c \right) \end{aligned} \qquad (6)$$

The main property of this formulation is that the contribution of each linear constraint is additive both in the numerator and in the denominator of (5). Thus, the introduction of new constraints is easy: one only needs to calculate the corresponding terms Γ_c and γ_c with (6).

An iterative algorithm to minimize R^* is obtained by successively updating φ for every node α according to:

$$\begin{aligned} \varphi^{(n+1)}(\alpha) &= -\frac{\Gamma^{*(n)}(\alpha) + \sum_c \Gamma_c^{(n)}(\alpha)}{M^*(\alpha) + \sum_c \gamma_c(\alpha)} \\ \varphi^{(n+1)}(\beta) &= \varphi^{(n)}(\beta) \quad \text{for } \beta \neq \alpha \end{aligned} \qquad (7)$$

We say that one iteration of DSI is accomplished when all the nodes of Ω have been scanned, which correspond to N elementary iterations. The main result concerning DSI is the following uniqueness and convergence property:

If φ is known on at least one node or if there is one non-null linear constraint, then $R^*(\varphi)$ has a unique minimum and the DSI algorithm converges to this minimum.

The proof can be found in [9]. It must be noticed that uniqueness is mainly due to the roughness criterion, which can be written $R(\varphi) = \varphi^T \mathbf{W} \varphi$, where $\mathbf{W}$ is a symmetric positive semi-definite matrix whose rank is $N - 1$. Moreover the algorithm in (7) is equivalent to a Gauss-Seidel method for solving the linear system:

$$(\mathbf{W} + \sum_c \varpi_c^2 \mathbf{A}_c^T \mathbf{A}_c)\varphi = \sum_c \varpi_c^2 \mathbf{A}_c^T b_c \qquad (8)$$

3.2. Application to the tomography problem

We now address the reconstruction problem defined in section 2. Let Ω be the set of voxels of the algebraic formulation, and G the graph for the 6-neighbours connectivity. The reconstruction problem can be seen as the construction of a smooth density function $\mathbf{f}$ which respects the linear system $\mathbf{Y} = \mathbf{Hf}$ as well as possible. We can consider the ray equations in (1) as linear constraints, all having the same weight ϖ. The criterion to be minimized is then:

$$R^*(\mathbf{f}) = R(\mathbf{f}) + \varpi^2 \left\| \mathbf{Y} - \mathbf{Hf} \right\|^2 \qquad (9)$$

To be consistent with the previous notations, we now denote $f(i)$ as well as f_i the i^{th} component of $\mathbf{f}$. The i^{th} equation is $\mathbf{h_i f} = y_i$ and, by use of (6), it leads to two additive terms in the DSI iterative formula at voxel α:

$$\begin{array}{rcl} \gamma_i(\alpha) & = & \varpi^2 h_{i\alpha}^2 \\ \Gamma_i(\alpha) & = & \varpi^2 h_{i\alpha}(\sum_{j \neq \alpha} h_{ij} f(j) - y_i) \end{array} \qquad (10)$$

Note that if we call $\mathbf{g}_\alpha$ the volume null everywhere except in voxel α where $\mathbf{g}_\alpha(\alpha) = 1$, we have the following equality:

$$\sum_i h_{i\alpha}^2 = [\mathbf{H}^T(\mathbf{Hg}_\alpha)]_\alpha \qquad (11)$$

$\mathbf{H}^T$ is the backprojection operator: it sets the value of a voxel to the sum of the corresponding densities on the projections. $\mathbf{Hg}_\alpha$ represents the reprojected images of $\mathbf{g}_\alpha$. Therefore, in our problem, the value of $\mathbf{H}^T(\mathbf{Hg}_\alpha)$ in voxel α can be replaced by the number P of X-ray projections. If we denote $\delta^{(n)}(\alpha) = \sum_i h_{i\alpha}(y_i - \mathbf{h_i f}^{(n)})$ the residual for voxel α, by substituting (10) in (7) for all rays and use of (11), we obtain the DSI update formula for tomography:

$$f^{(n+1)}(\alpha) = -\frac{\Gamma^{*(n)}(\alpha) - \varpi^2(P f^{(n)}(\alpha) + \delta^{(n)}(\alpha))}{M^*(\alpha) + \varpi^2 P} \qquad (12)$$

The main difference with ART-like algorithms is that each iteration acts on one voxel instead of acting on one ray. Moreover, if the roughness terms M^* and Γ^* are removed from (12), the iteration is identical to ICM (Iterated Conditional Modes), recently proposed by Payot [10] for vessels reconstruction.

3.3. Additional constraints

Regularizing the inverse problem with a smoothness function is sufficient to insure convergence and uniqueness of the method. Nevertheless, one may want to insert more prior knowledge in the model. In this subsection, we describe four constraints that can be added to change the aspect of the solution without losing the properties of the method.

Positivity. This constraint can be used when the reconstructed volume is known to be positive. Then, as it is usually done with ART, each voxel is forced to remain positive at update time.

Closeness to a given volume. The solution can be constrained to stay close to a given volume $\mathbf{f}^*$. This is incorporated in DSI as N linear constraints $f(i) - f^*(i) = 0$, all having the same weight ϖ_s. Each constraint only acts on one voxel, so there are two extra terms in the iterative formula which are $\gamma_s = \varpi_s^2$ and $\Gamma_s(\alpha) = -\varpi_s^2 f^*(\alpha)$.

Minimal variance. In the DSI formulation, inserting the variance $V(\mathbf{f})$ in the minimized criterion is equivalent to adding N linear constraints $f(i) - \overline{f} = 0$ with the same weight ϖ_v. The calculation of the global contributions γ_v and Γ_v from (6) leads to $\gamma_v = \varpi_v^2 \frac{N-1}{N}$ and $\Gamma_v(\alpha) = \varpi_v^2(-\sum_{j \neq \alpha} \frac{f(j)}{N})$

Minimal total density. The square of the total volume density $S(\mathbf{f})$ can also be inserted in the criterion. This corresponds to the addition of a single constraint $\sum_i f(i) = 0$, weighted by ϖ_d. This induces, for a voxel α: $\gamma_d = \varpi_d^2$ and $\Gamma_d(\alpha) = \varpi_d^2 \sum_{j \neq \alpha} f(j)$.

Finally, merging all those constraints leads to the following algorithm:

$$\begin{array}{l} \hat{f}^{(n+1)}(\alpha) = \\ -\frac{\Gamma^{*(n)}(\alpha) + \sum_i \Gamma_i^{(n)}(\alpha) + \Gamma_s(\alpha) + \Gamma_v^{(n)}(\alpha) + \Gamma_d^{(n)}(\alpha)}{M^*(\alpha) + \varpi^2 P + \gamma_s + \gamma_v + \gamma_d} \\ f^{(n+1)}(\alpha) = \max(\hat{f}^{(n+1)}(\alpha), 0) \end{array} \qquad (13)$$

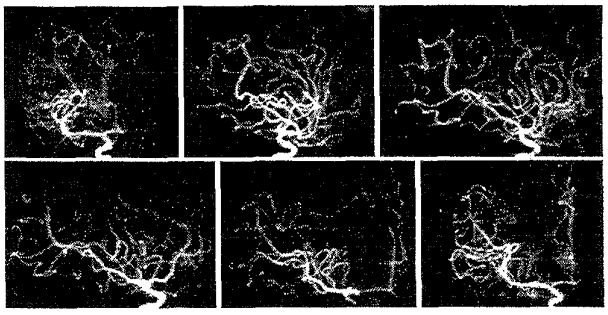

Figure 1. Six angiographic projections of an internal carotid artery

which converges to the unique positive minimum of:

$$R(\mathbf{f})+\varpi^2||\mathbf{Y}-\mathbf{Hf}||^2+\varpi_s^2||\mathbf{f}-\mathbf{f}^*||^2+\varpi_v^2 V(\mathbf{f})+\varpi_d^2 S(\mathbf{f})^2 \quad (14)$$

4. Application to 3D vascular reconstruction

In this section, our algorithm is compared to other algebraic methods for reconstruction of an internal carotid artery from six DSA images. The projections (see Fig. 1) were extracted from three biplane angiographic sequences acquired in stereotactic conditions. Images were corrected from geometric distortions through an accurate calibration and correction technique [6], and the projection matrices were computed using the fiducial markers of the stereotactic frame.

4.1. Reconstruction results

All experiments were made using the positivity constraint; it is a natural assumption in vascular reconstruction. One iteration of DSI is almost as much time-consuming as one cycle of ART or MART, but more iterations are needed for obtaining convergence. The initial volume has an influence over the number of iterations until convergence, but not over the final solution, since it is unique. We chose to initialize the volume with a null value. We stopped DSI after six iterations and ART after two or three. A normalized weight for X-ray equations constraint is defined as $\omega = (\varpi^2 P)/M^*(\alpha)$, so that when $\omega = 1$, the roughness term and the linear system term are equal in the denominator of (12).

Fig. 3.c shows the result of a DSI reconstruction with $\omega = 1.5$ and without other additional constraint. The solution satisfies very well the linear system (low reprojection error) but, as can be seen on the axial slice, the reconstructed volume suffers from a lack of uniformity. The minimal variance constraint can be used to add a regularization effect on the solution. The normalized weight is in this case $\omega_v = \varpi_v^2(N-1)/(NM^*(\alpha))$. Such experiments were made and unsurprisingly led to reconstructions very similar to the ART solution.

The constraint of minimizing the distance to a given volume $\mathbf{f}^*$ is only interesting in the case where a prior solution is known. Unfortunately, this not often the case, especially when dealing with images containing pathologies. The corresponding normalized weight is $\omega_s = \varpi_s^2/M^*(\alpha)$. Since a vascular volume is made of a large majority of black voxels, the algorithm could be used with $\mathbf{f}^* = 0$, but the reconstructed volume is once again very similar to the ART solution. In this case, a quadratic norm minimization is performed during the reconstruction.

A constraint was presented in section 3.3 where the sum of the densities in the volume is minimized. The normalized weigth can be taken as $\omega_d = (N/N_r)\varpi_d^2/M^*(\alpha)$, where N_r is the approximate number of voxels composing one ray equation, i.e. the number of non-null elements in a line of matrix $\mathbf{H}$. When $\mathbf{f}$ is positive, such a minimization tends to find a solution with a low L_1 norm and does not keep the average volume density (Fig. 4). Fig. 3.d shows the reconstruction obtained using $\omega = 1.5$ and $\omega_d = 1.5$. Compared to DSI without additional constraint, the quality has significantly improved: more vessels can be seen on the reconstruction. Moreover, the contrast on small vessels seems a little better than in the MART reconstruction and the artifacts due to occluding objects are avoided (see Fig. 2).

4.2. Discussion

We have presented a flexible iterative method for reconstructing an object from its projections which is based on the DSI formulation. The algorithm minimizes a criterion composed of different linear terms whose weights change the aspect of the reconstructed volume. One of them is a roughness criterion which gives a smooth aspect to the solution. Its special form ensures the uniqueness of the solution and the convergence of the algorithm, even with noisy data. Implementation of the method leads to a voxel by voxel algorithm behaviour instead of the classical ray by ray methods. Its application for cerebral vascular reconstruction from a few number of projections shows promising results, especially when the total volume density is inserted in the minimized criterion.

References

[1] J.-L. Coatrieux, M. Garreau, R. Collorec, and C. Roux. Computer vision approaches for the three-dimensional re-

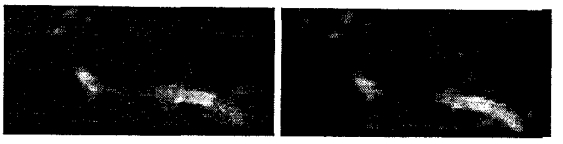

Figure 2. Zoom of a coronal slice: MART (left) and DSI (right) reconstructions. A vessel is uncomplete with MART because it is partially invisible in projection 5.

construction of coronary arteries: Review and prospects. *Crit. Rev. in Biomed. Eng.*, 22(1):01–38, 1994.

[2] M. Garreau, J.-L. Coatrieux, R. Collorec, and C. Chardenon. A knowledge-based approach for 3-d reconstruction and labeling of vascular networks from biplane angiographic projections. *IEEE Trans. on Med. Im.*, 10(2):122–131, 1991.

[3] G. T. Herman. *Image Reconstruction from Projections: the Fundamentals of Computerized Tomography*. Academic Press, New York, 1980.

[4] G. T. Herman, A. Lent, and S. W. Rowland. ART: Mathematics and Applications. *J. of Theor. Biol.*, 42:1–32, 1973.

[5] H. C. Kim, B. G. Min, T. S. Lee, S. G. Lee, C. W. Lee, J. H. Park, and M. C. Han. 3-d digital subtraction angiography. *IEEE Trans. on Med. Im.*, MI-1(2):152–158, 1982.

[6] L. Launay, C. Picard, E. Maurincomme, R. Anxionnat, P. Bouchet, and L. Picard. Quantitative evaluation of an algorithm for correcting geometrical distortions in dsa images: applications to stereotaxy. In *SPIE Medical Imaging*, volume 2434, pages 520–530, San Diego, 1995.

[7] A. Lent. A convergent algorithm for maximum entropy image restoration, with a medical x-ray application. In *Image Analysis and Evaluation*, pages 249–257. Soc. of Photo. Sci. and Eng., 1977.

[8] J.-L. Mallet. Dicrete smooth interpolation. *ACM Trans. Graph.*, 8(2):121–144, 1989.

[9] J.-L. Mallet. Discrete smooth interpolation in geometric modelling. *Computer Aided Design*, 24(4):177:191, 1992.

[10] E. Payot, F. Prêteux, R. Guillemaud, and Y. Trousset. Adaptive markovian model for 3d x-ray vascular reconstruction. In *SPIE conf. neur., morph., and stoch. meth. in im. and sig. Proc.*, San-Diego 1995.

[11] C. Pellot, A. Herment, M. Sigelle, P. Horain, H. Maitre, and P. Peronneau. 3d reconstruction of vascular structures from two x-ray angiograms using an adapted simulated annealing algorithm. *IEEE Trans. on Med. Im.*, 13(1):48–60, 1994.

[12] Y. Sun, I. Liu, and J. K. Grady. Reconstruction of 3d binary tree-like structures from three mutually orthogonal projections. *IEEE Trans. on Patt. Anal. and Mach. Intell.*, 16(3):241–248, 1994.

[13] D. Terzopoulos, A. Witkin, and M. Kass. Constraints on deformable models: recovering 3d shape and nonrigid motion. *Artificial Intelligence*, 36:91–123, 1988.

[14] Y. Trousset, D. Saint-Felix, A. Rougée, and C. Chardenon. Multiscale cone-beam x-ray reconstruction. In *SPIE Medical Imaging*, volume 1231, pages 229–238, 1990.

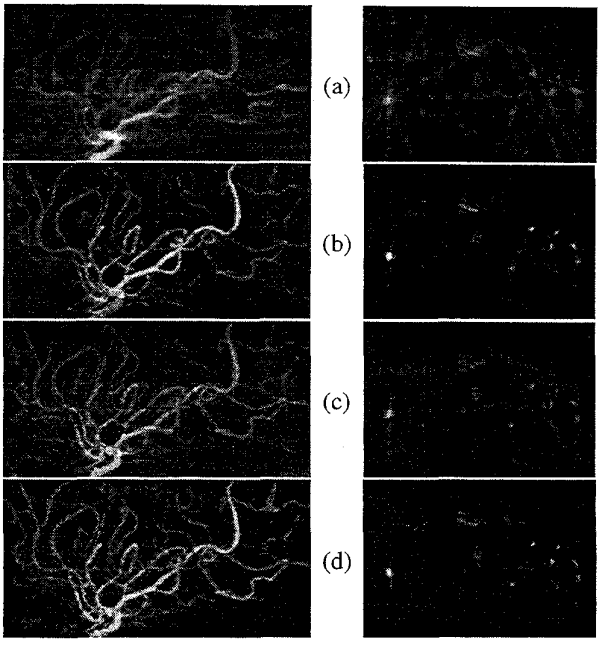

Figure 3. Comparison of (a) ART, (b) MART, (c) DSI with $\omega = 1.5$ and (d) DSI with $(\omega = 1.5, \omega_d = 1.5)$. Left: 3D views, right: axial slices.

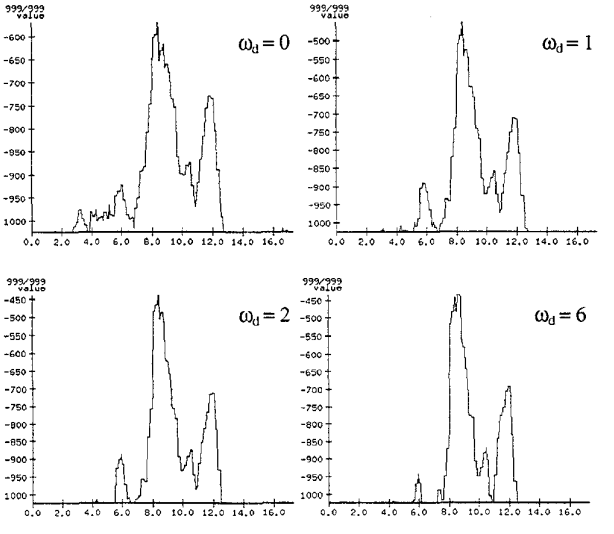

Figure 4. Effect of minimizing the total density in the volume. Density profiles of a segment extracted from DSI reconstructions with different ω_d weights. The noise part of the curve disappears, while the peaks are preserved.